

# The High-Resolution Crystal Structure of a 24-kDa Gyrase B Fragment From *E. coli* Complexed With One of the Most Potent Coumarin Inhibitors, Clorobiocin

Francis T.F. Tsai,<sup>1</sup> Onkar M.P. Singh,<sup>2</sup> Tadeusz Skarzynski,<sup>2</sup> Alan J. Wonacott,<sup>2</sup> Simon Weston,<sup>3</sup> Alec Tucker,<sup>3</sup> Richard A. Pauptit,<sup>3</sup> Alexander L. Breeze,<sup>3</sup> J. Philip Poyser,<sup>4</sup> Ronan O'Brien,<sup>5</sup> John E. Ladbury,<sup>5</sup> and Dale B. Wigley<sup>1\*</sup>

<sup>1</sup>Laboratory of Molecular Biophysics, University of Oxford, Oxford, United Kingdom

<sup>2</sup>Department of Biomolecular Structure, Glaxo Wellcome Research and Development Ltd., Medicine Research Centre, Stevenage, United Kingdom

<sup>3</sup>Protein Structure Laboratory, Zeneca Pharmaceuticals, Macclesfield, United Kingdom

<sup>4</sup>Target Discovery & Infection, Zeneca Pharmaceuticals, Macclesfield, United Kingdom

<sup>5</sup>Department of Biochemistry and Molecular Biology, University College London, London, United Kingdom

**ABSTRACT** Coumarin antibiotics, such as clorobiocin, novobiocin, and coumermycin A1, inhibit the supercoiling activity of gyrase by binding to the gyrase B (GyrB) subunit. Previous crystallographic studies of a 24-kDa N-terminal domain of GyrB from *E. coli* complexed with novobiocin and a cyclothialidine analogue have shown that both ligands act by binding at the ATP-binding site. Clorobiocin is a natural antibiotic isolated from several *Streptomyces* strains and differs from novobiocin in that the methyl group at the 8 position in the coumarin ring of novobiocin is replaced by a chlorine atom, and the carbamoyl at the 3' position of the noviose sugar is substituted by a 5-methyl-2-pyrrolylcarbonyl group. To understand the difference in affinity, in order that this information might be exploited in rational drug design, the crystal structure of the 24-kDa GyrB fragment in complex with clorobiocin was determined to high resolution. This structure was determined independently in two laboratories, which allowed the validation of equivalent interpretations. The clorobiocin complex structure is compared with the crystal structures of gyrase complexes with novobiocin and 5'-adenylyl- $\beta$ , $\gamma$ -imidodiphosphate, and with information on the bound conformation of novobiocin in the p24-novobiocin complex obtained by heteronuclear isotope-filtered NMR experiments in solution. Moreover, to understand the differences in energetics of binding of clorobiocin and novobiocin to the protein, the results from isothermal titration calorimetry are also presented. *Proteins* 28:41–52, 1997 © 1997 Wiley-Liss, Inc.

**Key words:** type II topoisomerase; gyrase; coumarin inhibitor; clorobiocin

## INTRODUCTION

Bacterial DNA gyrase is a type II topoisomerase, which uniquely catalyzes the negative supercoiling of closed-circular DNA using the free energy released by ATP hydrolysis.<sup>1–3</sup> The biological significance of this enzyme in many vital cellular processes and its unique presence in prokaryotes makes it an attractive drug target. Coumarin antibiotics, such as clorobiocin and novobiocin (Fig. 1), are natural compounds that have been isolated from *Streptomyces*.<sup>4</sup> The compounds target the gyrase B subunit and inhibit the ATPase reaction.<sup>1,5,6</sup>

A comparison of coumarins and their analogues led to the identification of important structural features essential for gyrase inhibition.<sup>7,8</sup> These inhibitors have a 4-hydroxycoumarin core in common, which is substituted at the 7 and 3 positions. Unsubstituted coumarins and noviose sugars lack detectable inhibitory activity. The substitution of a 3'-noviose carbamoyl (novobiocin) for a 5-methyl-2-pyrrolylcarbonyl group (clorobiocin) results in an enhancement of the inhibition of gyrase in vitro.<sup>7</sup> Furthermore, a comparison of the ability of clorobiocin and novobiocin to inhibit the DNA supercoiling reaction and bacterial growth revealed substantial differences in the relative coumarin concentrations required in vitro and in vivo.<sup>4,7</sup>

Lewis and colleagues<sup>9</sup> recently reported the crystal structures of a 24-kDa N-terminal GyrB fragment (p24) from *E. coli* complexed with novobiocin and a cyclothialidine analogue. The novobiocin complex has been solved at 2.7 Å resolution and confirmed that coumarins are competitive inhibitors of the ATPase activity. This is surprising, since there is little structural similarity between ATP and the

\*Correspondence to: Dr. Dale B. Wigley, Laboratory of Molecular Biophysics, Rex Richards Building, University of Oxford, South Parks Road, Oxford OX1 3QU, U.K.  
E-mail: wigley@biop.ox.ac.uk

Received 9 September 1996; Accepted 4 November 1996

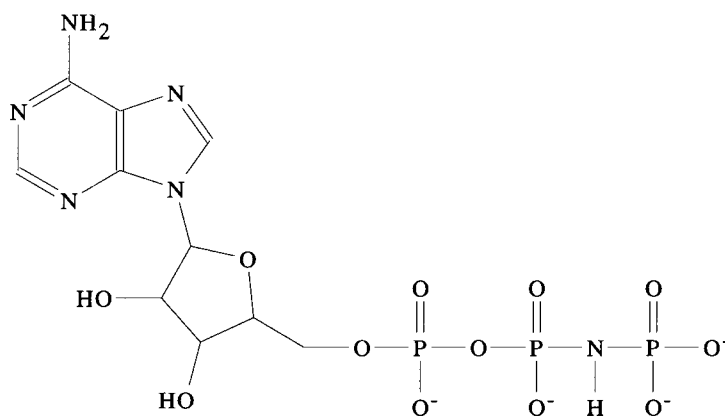
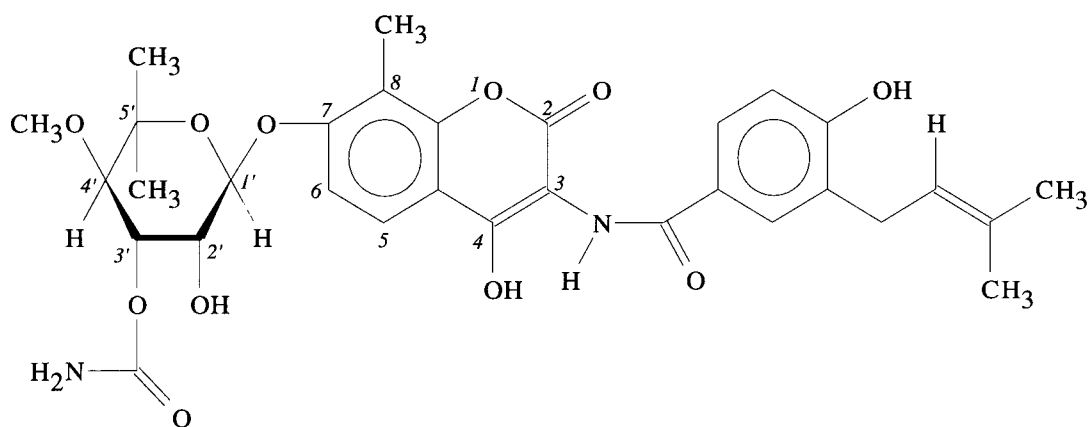
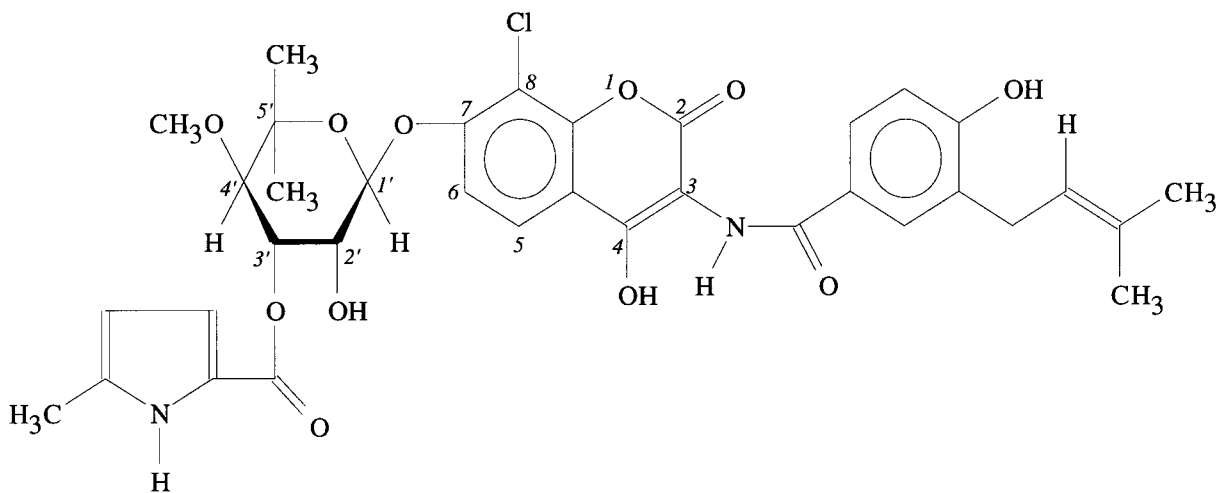


Fig. 1. Chemical structures of gyrase B inhibitors.

drug. The orientation of the coumarin ring was difficult to establish with certainty, and the conformation of the noviose sugar was not absolutely clear at this resolution.

We report here the high-resolution crystal structure of p24 complexed with one of the most potent coumarin inhibitors—clorobiocin. The crystals of the clorobiocin complex diffract to beyond 1.9 Å, and the

structure determination was carried out independently in two laboratories. The p24-clorobiocin structure is also compared to that of the p24-novobiocin<sup>9</sup> and the 43-kDa GyrB fragment complexed with ADPNP.<sup>10</sup> To understand the nature of the different inhibitory potencies of clorobiocin and novobiocin, we determined the thermodynamic parameters of the clorobiocin and novobiocin complexes, respectively, by using isothermal titration calorimetry (ITC). These data are also presented here. Finally, in order to address the question of possible influences of crystal contacts on the bound conformation of coumarin inhibitors, isotope-filtered NMR experiments of the novobiocin complex in solution were also performed.

## MATERIALS AND METHODS

### Crystallization

At Oxford, the protein was crystallized in the presence of 0.1–0.2 mM clorobiocin (in methanol) by the hanging drop vapor diffusion method at 21°C. Needle crystals of diffraction quality appeared routinely after 2 to 3 days and reached a maximum size of 0.60 mm × 0.25 mm × 0.10 mm after 2 to 4 weeks. For crystallization, 2–3  $\mu$ L of protein (4–6 mg mL<sup>-1</sup>) in 20 mM Tris/HCl pH 7.7, 1 mM EDTA, and 1 mM DTT were mixed with an equal volume of well solution. The latter consisted of 6–7% methoxy-PEG 2000, 8% isopropanol, and 100 mM MES/NaOH pH 5.7.

At Zeneca, clorobiocin was solubilized by conversion to the sodium salt by titration of a 75% acetone/water solution with 0.1 N NaOH, careful removal of the acetone by evaporation, and any solid precipitate by centrifugation, after which the supernatant could be used with Tris/HCl pH 8. Crystals were grown essentially as described above.

### Data Collection and Processing

The crystals belong to the orthorhombic space group P2<sub>1</sub>2<sub>1</sub>2<sub>1</sub> and diffract to beyond 1.9 Å using synchrotron radiation. Complete data were collected at room temperature (Oxford/Glaxo) and at 5°C (Zeneca) on a 30 cm MARresearch image plate mounted on station 9.6 at the Synchrotron Radiation Source (SRS), Daresbury, U.K. The results from these data collections are summarized in Table I.

The Oxford/Glaxo data were indexed and integrated by using the program DENZO,<sup>11</sup> and then postrefined with SCALEPACK.<sup>11</sup> Zeneca data were processed by a version of MOSFLM adapted for use with Image Plate data (A. Leslie, personal communication). In both cases, the integrated data were scaled, merged, and reduced to the unique data set using the CCP4 suite of programs.<sup>12</sup>

## Structure Determination

### p24-clorobiocin (Oxford/Glaxo)

The crystals were isomorphous to those of the p24-novobiocin complex, which allowed the calculation of difference electron density maps using phases derived from the protein part of the p24-novobiocin structure.<sup>9</sup> Before refinement, 5% of the data were randomly selected and used to calculate the Free- $R_{\text{cryst}}$  ( $R_f$ ) value.<sup>13</sup> Rigid-body refinement of the p24-clorobiocin model against 95% of the data between 10 Å and 1.9 Å, using X-PLOR,<sup>14</sup> reduced the initial  $R_{\text{cryst}}$  value from 40.8% ( $R_f$  = 41.6%) to 40.7% ( $R_f$  = 41.5%). The protein was refined initially in the absence of the inhibitor by using a combination of conventional least-squares refinement<sup>15</sup> and molecular dynamics x-ray refinement (X-PLOR).<sup>14</sup> This was interspersed with manual fitting of the model to electron density maps by using the program Turbo-Frodo.<sup>16</sup> In the final stages of the refinement, clorobiocin and solvent molecules were included in the model. The chemical structure of clorobiocin was modeled from the energy minimized structure of novobiocin using the program QUANTA Version 4.0 (Molecular Simulations).

### p24-clorobiocin (Zeneca)

Direct Fourier synthesis was performed with calculated phases obtained from the protein part of the p24-novobiocin structure (unpublished data). The maps obtained contained clear density representing clorobiocin. Molecular replacement, using data between 8 Å and 3 Å, was also carried out to verify this structure solution: a search model comprising residues 23–220 of the 43-kDa DNA GyrB fragment was used in conjunction with the program AMoRe<sup>17</sup> to obtain a solution with a posttranslation function  $R$  factor of 44.2%, which rigid-body refinement reduced to 42.1%. This model formed the starting point for model building with FRODO.<sup>18</sup> Cycles of refinement, using data between 20 and 2.1 Å, were performed with the TNT least-squares refinement software package.<sup>19</sup>

## NMR Spectroscopy

The p24 protein, uniformly labeled (>98%) with <sup>15</sup>N and <sup>13</sup>C, was produced by overexpression in *E. coli* in the presence of minimal medium containing <sup>15</sup>N ammonium chloride and U-<sup>13</sup>C glucose as the sole nitrogen and carbon sources. Stoichiometric complexes of <sup>15</sup>N,<sup>13</sup>C-p24 with novobiocin were prepared in 20 mM sodium phosphate, pH 6.8, 50 mM NaCl, 5 mM MgCl<sub>2</sub>, 1 mM DTT, 0.01% (w/v) NaN<sub>3</sub>, and 8% (v/v) D<sub>2</sub>O. Samples contained 1.4 mM complex in 0.55 mL volume.

NMR spectra of the <sup>15</sup>N,<sup>13</sup>C-p24-novobiocin complex were acquired at 25°C on a 3-channel Varian Unity 600 MHz spectrometer equipped with a pulsed-field  $z$ -gradient unit. For assignment of <sup>1</sup>H resonances of the unlabeled novobiocin in the complex,

**TABLE I. Summary of Data Analysis**

a) Summary of data collection.					
Structure	p24-clorobiocin (Oxford/Glaxo)		p24-clorobiocin (Zeneca)		
Space Group	P2 <sub>1</sub> 2 <sub>1</sub> 2 <sub>1</sub>		P2 <sub>1</sub> 2 <sub>1</sub> 2 <sub>1</sub>		
Cell Dimensions (Å)	<i>a</i> = 40.82, <i>b</i> = 47.96, <i>c</i> = 111.77		<i>a</i> = 40.81, <i>b</i> = 48.00, <i>c</i> = 112.27		
Number of Crystals	4		1		
No. of frames collected	75		40		
Oscillation	1°–2°		2°		
Resolution	1.9		2.1		
Overall Completeness	91.3%		91.6%		
Mean I/σI <sup>§</sup>	6.1		7.4		
R <sub>svm</sub> <sup>†</sup>	0.058		0.042		
Total reflections	53,076		35,038		
Unique reflections	16,411		12,316		
Multiplicity	3.2		2.8		
Temperature <sup>‡</sup>	21°C		5°C		
b) Effective resolution of data (Oxford/Glaxo).					
Resolution (Å)	No. of reflections	I/σI <sup>§</sup>	R <sub>svm</sub> (I) <sup>†</sup> (%)	Completeness (%)	Multiplicity
>7.31	264	6.7	5.7	83.7	3.6
4.67	510	7.2	5.2	97.3	4.4
4.10	572	9.6	5.1	95.4	4.4
3.40	715	8.5	5.7	98.6	4.4
2.96	823	9.0	6.4	99.3	3.8
2.66	885	13.1	4.9	96.6	2.9
2.44	971	11.3	6.1	97.2	2.9
2.26	1027	10.0	6.9	95.3	3.0
2.12	1101	7.1	9.7	96.0	3.0
2.00	1097	5.0	14.7	90.3	3.0
1.95	886	5.0	15.0	70.8	2.3
1.90	786	3.7	19.8	61.7	2.2
c) Effective resolution of data (Zeneca).					
Resolution (Å)	No. of reflections	I/σI <sup>§</sup>	R <sub>svm</sub> (I) <sup>†</sup> (%)	Completeness (%)	Multiplicity
>6.33	530	5.5	2.7	98.5	2.7
4.60	824	30.3	1.9	98.6	2.9
3.79	1039	28.7	2.3	100.0	2.8
3.29	1191	24.6	2.8	98.8	2.8
2.95	1305	16.4	4.5	97.3	2.8
2.70	1393	11.2	6.8	94.5	2.8
2.50	1436	8.2	9.3	90.4	2.8
2.34	1492	6.4	11.8	88.3	2.8
2.21	1550	5.1	15.0	86.1	2.9
2.10	1556	3.7	20.7	82.1	3.0

<sup>§</sup>I is the intensity of the reflection.

<sup>†</sup>R<sub>sym</sub>(I) is the reliability index for comparing the intensity of symmetry related reflections;  $R_{\text{sym}}(I) = \sum \sum |I_i(hkl) - \langle I(hkl) \rangle| / \sum \sum I_i(hkl)$ .

<sup>‡</sup>Temperature at which data was collected.

and for extraction of intramolecular <sup>1</sup>H–<sup>1</sup>H nuclear Overhauser enhancements (NOEs) for the bound novobiocin, F<sub>1</sub>,F<sub>2</sub> (<sup>15</sup>N,<sup>13</sup>C)-isotope filtered (IF) 2D TOCSY (19 ms isotropic mixing time) and NOESY (75 ms NOE mixing time) NMR spectra were acquired as described in Breeze and colleagues.<sup>20</sup>

### ITC Analysis

ITC experiments were performed on an MCS calorimeter (MicroCal Inc., MA, USA). In a typical experiment, sixteen 15-μL injections of protein were added to 1.3 mL of drug in the calorimeter cell.<sup>21</sup>

Protein solutions were extensively dialyzed in buffer consisting of 20 mM Tris/HCl pH 7.5 and 1 mM EDTA before each experiment. The drug compounds were initially dissolved in ethanol and then diluted with buffer from the protein dialysate until the ethanol concentration was reduced to a minimum (typically 5% v/v). A similar percentage of ethanol was added to the solution containing protein. Due to the insolubility of the drug compounds they were put in the calorimeter cell, which allowed them to have a 10-fold lower concentration compared to the interacting component in the syringe. The concentration of

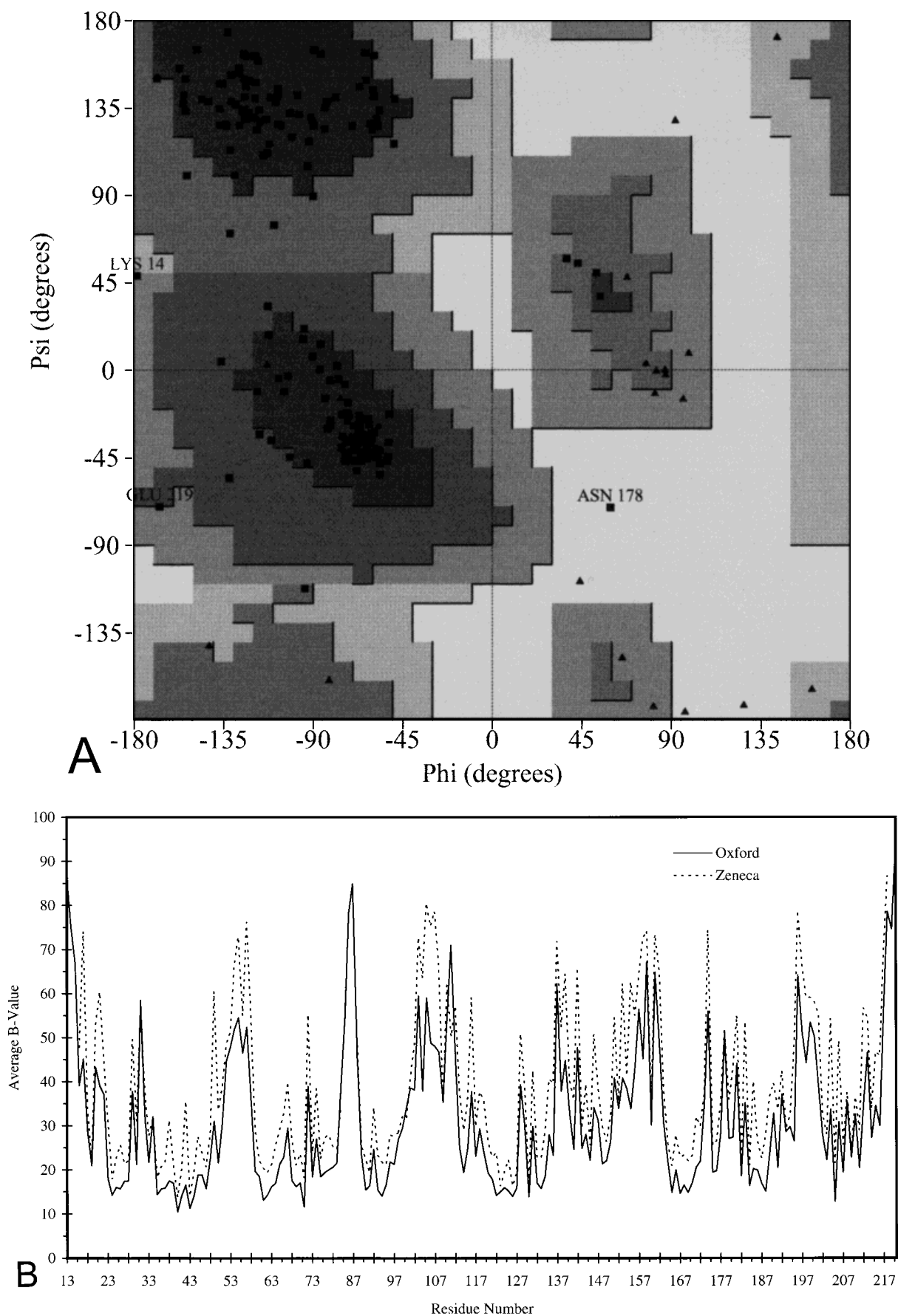


Fig. 2. **A:** Ramachandran plot for the p24-clorobiocin structure determined at Oxford/Glaxo. The favored, additional allowed, generously allowed, and disallowed regions are shown in different

gray tones, from dark gray to white, respectively. Glycine residues are shown as triangles and all other residues as squares. **B:** Graph of the average B values (Å<sup>2</sup>) for individual residues.

the protein was verified by measuring its  $A_{280}$ . The concentration of the drug was determined by weight alone, and where systematic errors were apparent this was allowed as a variable in titration curve-fitting procedures. Careful measurement of the large heats of dilution were made of both the interacting species by performing the titration of protein into buffer and buffer into drug. The resultant heats per injection were subtracted from the data for the drug/protein interaction. Data fitting was achieved as described elsewhere<sup>22</sup> using least-squares nonlinear curve-fitting to titration data to obtain values for the stoichiometry ( $N$ ), the equilibrium binding constant ( $K_B$ ), and the enthalpy change per mole of protein ( $\Delta H^\circ$ ). Full thermodynamic characterization of the interaction can be made based on the following relationship:

$$-RT \ln K_B = \Delta G^\circ = \Delta H^\circ - T \Delta S^\circ$$

where  $R$  is the gas constant,  $T$  is the absolute temperature,  $\Delta G^\circ$  is the change in free energy and  $\Delta S^\circ$  is the change in entropy on going from free to bound state.

## RESULTS

### Comparison of the Two p24-Clorobiocin Structures

The two independently solved structures are identical within experimental error. The root mean square deviation between equivalent  $C\alpha$  pairs and all protein atoms is 0.24 Å and 0.96 Å, respectively. Only occasional variations in side chain orientation could be detected, and none of these were considered significant. The difference maps for both structures contained clear electron density for the bound clorobiocin. In both structures, the N and C termini, as well as a loop region consisting of residues 83 to 86 (Oxford/Glaxo) and residues 81 to 87 (Zeneca) are disordered. The two equivalent, independent results are a clear indication of the validity of the structure determination and the correctness of the model. Figure 2a shows the Ramachandran plot for the Oxford/Glaxo structure generated by using the program PROCHECK.<sup>23</sup> The final model consisted of 204 residues and 104 solvent molecules. Almost 90% of the total number of residues are present in most favoured regions (Table II). Figure 2b shows a graph of the respective mean B factor values for all protein atoms plotted as a function of residue number. The refinement statistics for both structures are given in Table II.

### Description of the p24-Clorobiocin Complex

The overall protein fold of p24-clorobiocin is very similar to the equivalent region of the 43-kDa GyrB<sup>10</sup> and is depicted in Figure 3. The major conformational difference between the equivalent parts in both structures is found in a loop region consisting of

**TABLE II. Summary of Crystallographic Structure Analysis**

Structure	p24-clorobiocin (Oxford/Glaxo)	p24-clorobiocin (Zeneca)
Resolution range	10–1.9 Å	20–2.1 Å
Number of residues	204	196
Solvent molecules	104	57
$R_{\text{cryst}}^{\dagger}$	0.214	0.199
Free- $R_{\text{cryst}}^{\ddagger}$	0.287	—
Average B-factor (main chain)	27.51 Å <sup>2</sup>	30.74 Å <sup>2</sup>
Average B-factor (protein only)	28.50 Å <sup>2</sup>	37.07 Å <sup>2</sup>
r.m.s. deviation of ideal bond length	0.013 Å	0.015 Å
r.m.s. deviation of ideal bond angle	3.10°	1.18°
Residues in most favoured regions	89.7%	89.9%

r.m.s. = root mean square.

<sup>†</sup> $R_{\text{cryst}}$  = is the crystallographic residual factor indicating the correctness of a model structure;  $R_{\text{cryst}} = \sum |F_o| - k |F_c| / \sum |F_o|$ .

<sup>‡</sup>Free- $R_{\text{cryst}}$  = Cross validation residual factor using 5% of the native data, which were selected randomly and excluded from the refinement protocol (13).

residues 98 to 120, which has moved by up to 26 Å away from its position in the 43-kDa protein dimer. This loop movement is indicated in Figure 4, which shows the p24-coumarin complex superimposed with a p24-ADPNP model generated from the 43 kDa GyrB-ADPNP dimer.<sup>10</sup> For clarity only the residues of the ADPNP complex involved in loop movement are shown. In the “open” conformation, as seen in p24-clorobiocin, the ATP-binding site is exposed, in contrast to the “closed” conformation, as seen in the 43-kDa dimer.

The binding sites for clorobiocin and ATP are not identical, although they do overlap to some extent. A comparison of the p24-clorobiocin crystal structure with that of the 43-kDa GyrB fragment shows that the noviose sugar and the attached pyrrole ring of clorobiocin superimpose with the adenine ring and ribose of ATP, while the coumarin and isopentenyl group are in close proximity to the nucleotide-binding N-terminal arm from the other subunit in the 43-kDa fragment dimer.

The coumarin and the isopentenyl group are arranged around Pro 79 in such a way that the isopentenyl group folds back away from solvent onto the coumarin ring, neatly reducing the overall hydrophobic surface of the drug as well as forming hydrophobic interactions with the protein. This conformation has also been observed in the p24-novobiocin structure.<sup>9</sup> The question of whether this is likely to be a true bioactive conformation of coumarins or an artifact of crystal packing, since both novobiocin and clorobiocin are involved in direct polar lattice interactions in this crystal form, was addressed by NMR (see below).

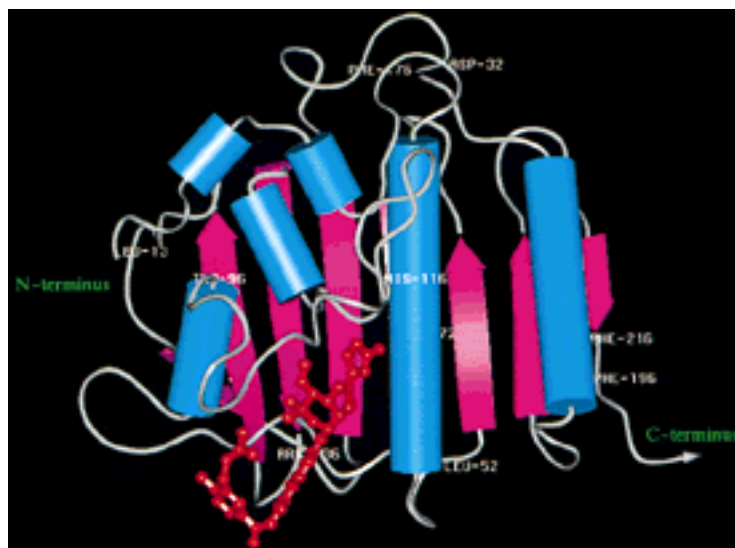


Fig. 3. Diagram, generated by using the program PREPPI, showing the overall fold of the 24-kDa N-terminal gyrase B fragment complexed with clorobiocin.  $\alpha$  helices are shown as cylinders (cyan) and  $\beta$  strands as arrows (magenta). The N and C

termini are indicated, and side chains are labeled periodically to facilitate chain tracing. The coumarin is overlaid in red as a ball-and-stick model.

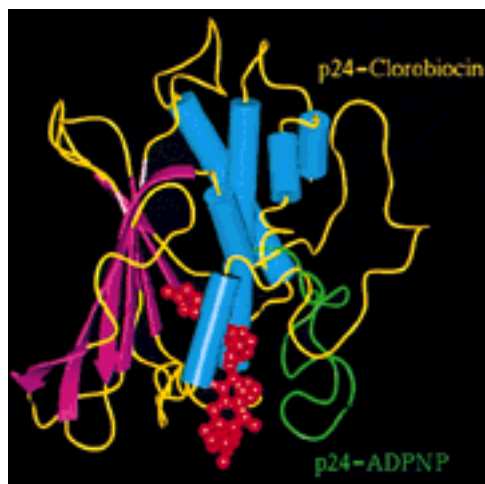


Fig. 4. Diagram illustrating the structural rearrangement of p24-clorobiocin with respect to p24-ADPNP. The clorobiocin complex (yellow, cyan, magenta) is superimposed onto the p24-ADPNP model (green). Clorobiocin is represented as a ball-and-stick model; ADPNP is not shown. For clarity only the residues of the p24-ADPNP model, which are involved in loop movement between the two protein complexes, are shown.

#### Details of the Interactions Made Between Clorobiocin and p24

Several close interactions between the coumarin inhibitor and the protein are observed. The most important interaction is probably that involving two hydrogen bonds from the Arg 136 side chain to the 2-coumarin carbonyl oxygen (2.9 Å and 2.9 Å), which are critical for the sensitivity of GyrB to coumarins.<sup>6,24-26</sup>

The other two direct protein–ligand hydrogen bonds of importance are those between the 2'-noviose hydroxyl and the carbonyl oxygen of Asn 46 (2.7 Å) and between the imino group of the pyrrole moiety and the Asp 73 side chain (2.8 Å). In addition, there are a number of hydrogen bonding interactions between clorobiocin and ordered solvent molecules.

The pyrrole ring sits in a hydrophobic pocket (Val 43, Val 71, Val 120, Val 167, and Ile 78), shown in Figure 5, and is embedded between Ala 47 and Tyr 165. This pocket is conserved in both the 43-kDa GyrB<sup>10</sup> and in the p24-novobiocin structure.<sup>9</sup> In both structures the pocket is occupied by two ordered water molecules,<sup>5</sup> which overlay with the 5-methyl-2-pyrrole ring of clorobiocin (Fig. 6). There are additional hydrophobic contacts against the coumarin ring and the isopentenyl group, for example, the Arg 76 side chain stacks against the ring, and there are contacts with Ile 78 and Ile 94. Thus, clorobiocin exploits both polar and apolar interactions upon binding.

#### Conformation of Novobiocin Bound to p24 in Solution by NMR

In the p24-novobiocin and p24-clorobiocin crystal structures the binding pocket for the inhibitor is located in a region of crystal contacts with a symmetry-related neighboring molecule. To address the question of whether the “folded” conformation seen for the inhibitors in the crystal structure is also adopted in solution, isotope-filtered solution NMR experiments were performed on the complex of novobiocin with uniformly <sup>15</sup>N and <sup>13</sup>C-labeled p24.

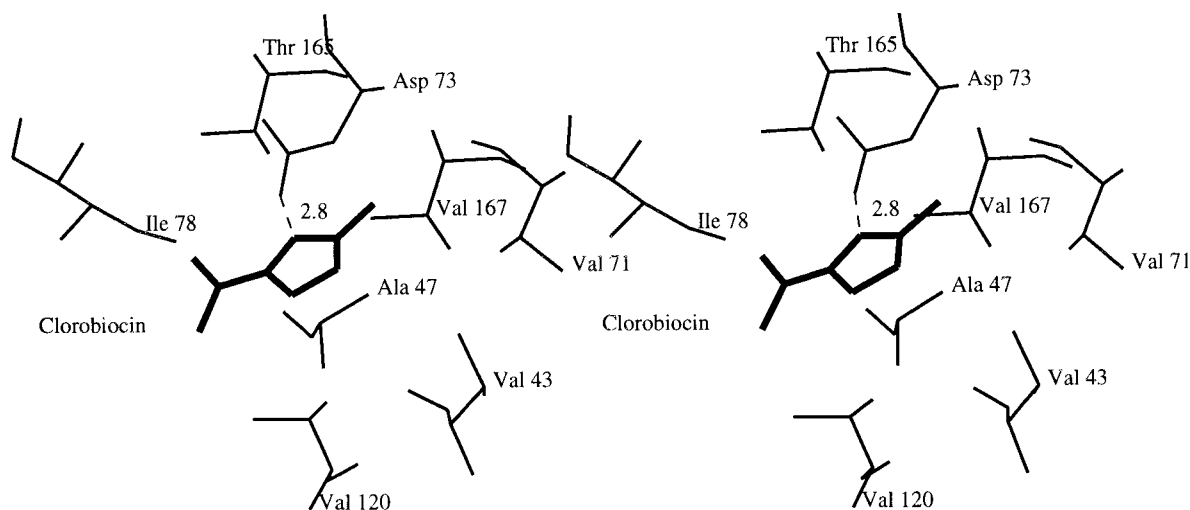


Fig. 5. Stereoscopic view of the clorobiocin pyrrole ring moiety located in the hydrophobic pocket. Protein residues aligning this hydrophobic pocket are shown.

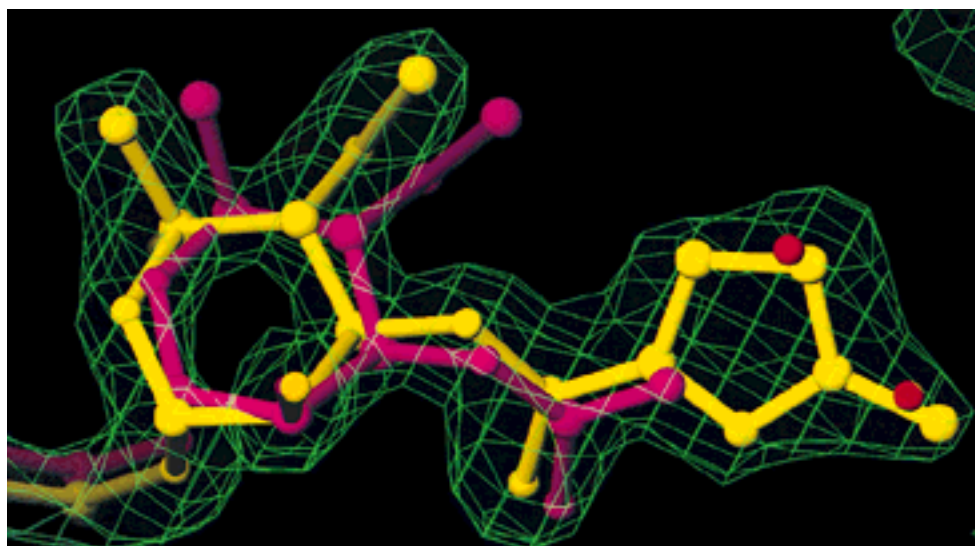


Fig. 6. Ball-and-Stick models of clorobiocin (yellow) and novobiocin (magenta) as seen in the crystal structures. The two water molecules, which are displaced in the p24-clorobiocin structure, are shown in red. The  $2F_o - F_c$  electron density map for the Oxford/Glaxo clorobiocin structure is contoured at  $1 \sigma$ .

The isotope-filtered data sets obtained for  $^{15}\text{N}$ ,  $^{13}\text{C}$ -p24-novobiocin were of good quality (Fig. 7b). Complete  $^1\text{H}$  assignments were obtained for the nonlabile protons and the peptide NH of the bound novobiocin by joint analysis of the IF-TOCSY and IF-NOESY spectra. For reference, Figure 7a shows a schematic diagram of the novobiocin structure in approximately the orientation seen in the crystal structure. A total of 31 structurally significant NOEs were identified from the IF-NOESY data set. Figure 7b shows a region of this spectrum containing NOEs whose presence restrain the relative orientation of the coumarin ring and the isopentenyl side chain.

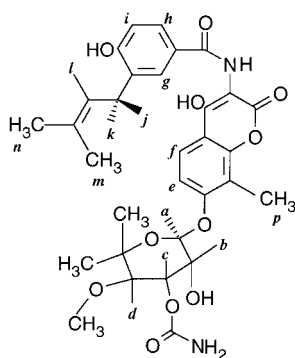
Collectively, these interactions confirm that the isopentenyl side chain is folded over to stack above the coumarin ring system in the complex in solution as well as in the crystal environment.

#### Thermodynamic Analysis of p24-Clorobiocin and p24-Novobiocin by ITC

ITC was used to determine the thermodynamic parameters involved in novobiocin and clorobiocin interactions with GyrB at  $17.5^\circ\text{C}$ . Initially, experiments were performed with the drug in 0.5% v/v ethanol; however, the clorobiocin was found to exhibit signs of association under these conditions, and



A



B

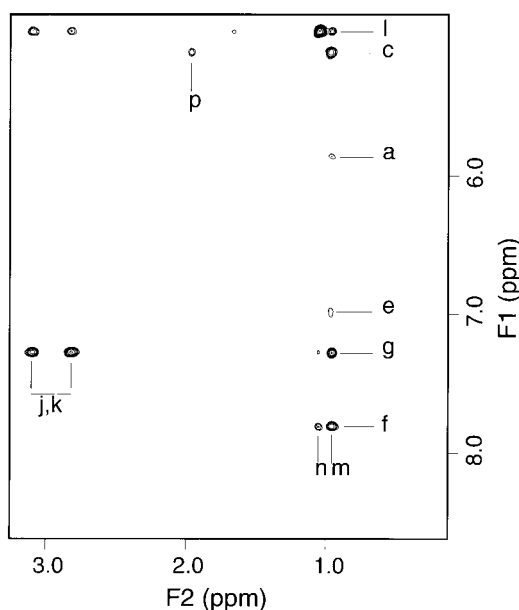


Fig. 7. **A:** Schematic diagram of novobiocin in the conformation adopted in the crystal structure. Protons involved in the major structurally significant NOE interactions are labeled in lowercase letters. **B:** Region of a 2D  $F_1$ ,  $F_2$  ( $^{15}\text{N}$ ,  $^{13}\text{C}$ )-IF-NOESY NMR spectrum (75 ms mixing time) of novobiocin bound to uniformly  $^{15}\text{N}$ ,  $^{13}\text{C}$ -labeled p24 in solution. The resonance positions of protons giving rise to NOE crosspeaks corresponding to some of the more important structurally restraining interactions are labeled as in Figure A. Presence of an NOE crosspeak implies an interproton distance of  $\approx 5$  Å.

reliable data could not be obtained. To circumvent this problem, 5% ethanol was adopted to allow comparison between the two drugs in subsequent experiments. This appeared to have little effect on the binding and hence on the protein conformation (see Materials and Methods).

As reported in a recent study<sup>27</sup> the binding of these drugs to GyrB are enthalpy driven at 25°C. The interactions of the two drugs are remarkably similar under the conditions used. Both the enthalpic and entropic parameters contribute favorably to the free

**TABLE III. Summary of Isothermal Titration Calorimetry Analysis**

Coumarin Complex	p24-clorobiocin	p24-novobiocin
Stoichiometry (N)	1 <sup>‡</sup>	1.12
Binding constant ( $K_B$ )	$2.28 (\pm 1.5) \times 10^7 \text{ M}^{-1}$	$4.07 (\pm 1.9) \times 10^7 \text{ M}^{-1}$
Gibbs Free Energy ( $\Delta G^\circ$ )	$-9785 \text{ cal mol}^{-1}$	$-10119 \text{ cal mol}^{-1}$
Enthalpy ( $\Delta H^\circ$ )	$-8790 (\pm 430) \text{ cal mol}^{-1}$	$-9303 (\pm 300) \text{ cal mol}^{-1}$
Entropy ( $T\Delta S^\circ$ )	$995 \text{ cal mol}^{-1}$	$816 \text{ cal mol}^{-1}$
Temperature	290.5 K	290.5 K

<sup>‡</sup>The clorobiocin concentration was floated for the purpose of fitting the titration to a 1:1 binding event.

energy of binding (Table III). The similarity of the thermodynamic data between the two drug interactions is of particular interest because two water molecules appear in the binding interface for the interaction of novobiocin, which are precluded by the binding of clorobiocin. However, the entropic gain expected for this displacement this is not reflected in a difference between the data for the two drugs.

## DISCUSSION AND CONCLUSIONS

### Structural Comparison of p24-Clorobiocin With p24-Novobiocin

A comparison of the p24-clorobiocin structure with that of p24-novobiocin reveals that the coumarin inhibitor-binding site is essentially the same for both complexes (Fig. 6). There is a slight rigid-body shift toward solvent ( $\leq 0.9$  Å) of the clorobiocin molecule with respect to the novobiocin location, which might be a result of steric effects necessary to accommodate the chlorine and the pyrrole ring.

The overlap of the coumarin and ATP-binding sites is consistent with coumarins being competitive inhibitors of the ATPase activity.<sup>28,29</sup> The most striking polar interactions made between p24 and clorobiocin are the hydrogen bonds between the Arg 136 side chain and the 2-coumarin carbonyl oxygen on clorobiocin. The isolation of spontaneous coumarin-resistant mutants of *E. coli* has revealed that Arg 136 is a key residue conferring coumarin resistance.<sup>6,24–26</sup>

The substitution of the 3'-carbamoyl in novobiocin for a 3'-(5-methyl-2-pyrrolylcarbonyl) as observed in clorobiocin, coumermycin A1, and other structurally related compounds results in a two- to sixfold increase in inhibitory activity.<sup>7</sup> Titration calorimetry has shown that the binding of the coumarins to p24 is enthalpy-driven.<sup>27</sup> A comparison of the p24-clorobiocin and p24-novobiocin structures revealed that the pyrrole moiety in clorobiocin, which sits in a hydrophobic pocket (Fig. 5), displaces two ordered water molecules. No conformational changes in the protein were apparent.

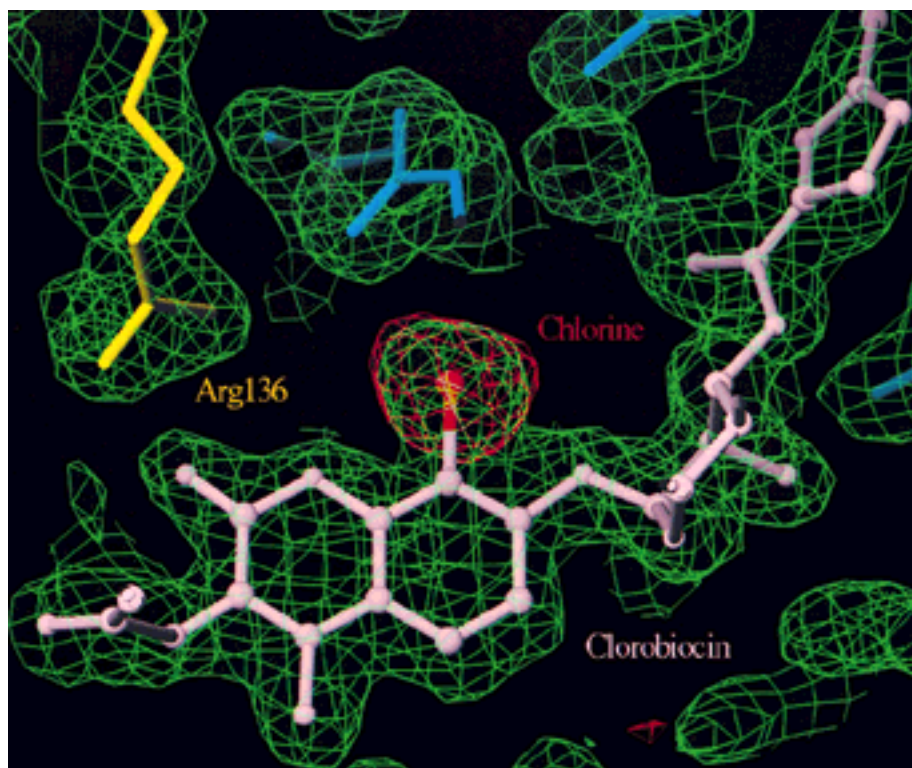


Fig. 8. The  $2F_o - F_c$  (green) and  $F_o - F_c$  (red) electron density maps for the Oxford/Glaxo p24-clorobiocin structure are contoured at  $1\sigma$  and  $3.5\sigma$ , respectively. Clorobiocin is shown in pink, Arg 136 in yellow, and all other protein residues in blue. The

chlorine atom (red) was omitted from the model in the calculation of the difference Fourier map. Parts of the isopentenyl group of clorobiocin have been omitted for clarity.

The difference in entropy due to the displacement of the two solvent molecules is not significant (Table III). These results are consistent with ITC results reported previously.<sup>27</sup> It has also been shown that the absence of the 5-methyl substituent on the pyrrole ring in coumermycin A1, results in a fourfold decrease in antibacterial activity,<sup>30</sup> suggesting that the additional hydrophobic interactions contribute to the binding of clorobiocin and coumermycin A1. Moreover, Berger and Batcho<sup>4</sup> have reported that the higher antibacterial potency of clorobiocin for bacterial growth is conferred by the 5-methylpyrrole moiety and not by the chlorine atom at the 8-coumarin position. Collectively, these results suggest that clorobiocin is a more potent antibiotic than novobiocin due to its increased cytotoxicity to *E. coli* and not because of more specific GyrB inhibition properties. This might be the direct result of a higher membrane permeability conferred by an increased hydrophobicity. Additional evidence for this hypothesis comes from a comparison study of clorobiocin and novobiocin to inhibit the DNA supercoiling reaction in vitro, and their inhibitory potency on *E. coli* growth.<sup>7</sup> Whereas only a twofold decrease in  $K_i$  is observed for clorobiocin in vitro, a near sixfold lower  $IC_{50}$  was found for this coumarin to inhibit bacterial growth.

The largest structural rearrangement between the p24-clorobiocin and the 43-kDa fragment ADPNP complex structures is the movement of a loop comprising residues 100 to 119. This loop is involved in phosphate binding in the 43-kDa GyrB fragment.<sup>10</sup> In the p24-clorobiocin structure the loop folds back, exposing the nucleotide-binding site and thereby may allow the binding of ATP. This is in contrast to the 43-kDa structure, in which the ADPNP molecule is "trapped" inside the protein via protein-nucleotide interactions,<sup>10</sup> suggesting that the binding of ATP to GyrB causes a conformational change within the protein. However, to date, no structural information exists on the apo-GyrB subunit. Hence it remains to be seen whether the protein conformation in the clorobiocin complex is identical to the apo-protein or represents an alternative conformation to accommodate the inhibitor.

### Conformation of Clorobiocin

The higher resolution analysis of the p24-clorobiocin complex confirms the orientation of the coumarin ring modeled into the lower resolution p24-novobiocin structure.<sup>9</sup> Figure 8 depicts the difference electron density for the chlorine atom at the 8-coumarin position in the clorobiocin, where novobiocin has a

methyl substituent. The position of the chlorine atom clearly establishes the relative orientation of the coumarin ring.

The noviose sugar moiety of clorobiocin has an energetically favorable chair conformation. This information was not clear from the medium resolution p24-novobiocin structure.<sup>9</sup>

The nonplanarity of the *cis*-amide bond between the coumarin and the benzamide is common to both complexes. Ultraviolet absorption spectroscopy and circular dichroism techniques have indicated previously that this amide bond is nonplanar.<sup>31</sup> Brand and Toribara<sup>31</sup> proposed that a conjugated, planar arrangement of the two aromatic systems would be sterically strained and therefore energetically unfavorable.<sup>31</sup> Furthermore, the NMR data indicate that the isopentenyl group does indeed fold over onto the coumarin ring, ruling out the influence of crystal packing forces. This conformation appears to be relevant for the binding of these ligands to gyrase and therefore for the inhibitory activity of coumarins.

Superimposing the p24-clorobiocin structure with that of the 43-kDa GyrB dimer indicates that parts of the inhibitors overlap with or are in very close proximity to the N-terminal arm in the 43-kDa GyrB dimer. Hooper and coworkers<sup>7</sup> reported that the addition of an alkyl side chain to the meta position of the hydroxybenzamide resulted in a tenfold increase in the inhibition of gyrase. These observations suggest two related modes of action for gyrase-specific coumarin inhibitors: occupation of the ATP site and prevention of dimerization by blocking access of the N-terminal arm.

#### ACKNOWLEDGMENTS

Oxford is grateful for support by Glaxo-Wellcome Research and Development Ltd. We thank Dr. P.J. Ritzkallah for help with the data collection on station 9.6 at the Synchrotron Radiation Source (SRS), Daresbury, U.K., Drs. H.S. Subramanya, P. Gouet, and I.D. Kerr for their help with structure refinement of p24-clorobiocin and generating a model for clorobiocin, and Dr. S. Islam and Professor M. Sternberg for providing their graphics program PREPPI. p24 used at Oxford was prepared at Leicester University and was a gift from Glaxo-Wellcome Research and Development Ltd. Clorobiocin was a kind gift from Rhône-Poulenc-Rorer to Glaxo-Wellcome Research and Development Ltd.

The protein used at Zeneca was prepared in-house by G. Rosenbrock by using a clone purchased from Leicester University. <sup>15</sup>N, <sup>13</sup>C-labeled p24 for NMR was produced at Zeneca by J. Stawpert. Zeneca is grateful for the gift of 10 mg of clorobiocin from Rhône-Poulenc-Rorer, and for the technical assistance of S. Nicholson in the preparation of the soluble clorobiocin sodium salt.

The atomic coordinates and structure factors will be deposited with the Brookhaven Protein Data Bank. F.T.F.T. is the recipient of a EPSRC-Glaxo-Wellcome Case Studentship, and D.B.W. is a BBSRC Advanced Fellow. J.E.L. is a Wellcome Trust Research Career Development Fellow.

#### REFERENCES

1. Reece, R.J., Maxwell, A. DNA gyrase: Structure and function. *Crit. Rev. Biochem. Mol. Biol.* 26:335-375, 1991.
2. Wigley, D.B. Structure and mechanism of DNA topoisomerases. *Annu. Rev. Biophys. Biomol. Struct.* 24:185-208, 1995.
3. Wang, J.C. DNA topoisomerases. *Annu. Rev. Biochem.* 54:665-697, 1996.
4. Berger, J., Batcho, A.D. Coumarins-glycoside antibiotics. *J. Chromatogr. Libr.* 15:101-158, 1978.
5. Lewis, R.J., Tsai, F.T.F., Wigley, D.B. Molecular mechanisms of drug inhibition of DNA gyrase. *BioEssays* 18:661-671, 1996.
6. Maxwell, A. The interaction between coumarin drugs and DNA gyrase. *Mol. Microbiol.* 9:681-686, 1993.
7. Hooper, D.C., Wolfson, J.S., McHugh, G.L., Winters, M.B., Swartz, M.N. Effects of novobiocin, coumermycin A1, clorobiocin, and their analogs on *Escherichia coli* DNA gyrase and bacterial growth. *Antimicrob. Agents Chemother.* 22:662-671, 1982.
8. Rádl, S. Structure-activity relationships in DNA gyrase inhibitors. *Pharmac. Ther.* 48:1-17, 1990.
9. Lewis, R.J., Singh, O.M.P., Smith, C.V., Skarzynski, T., Maxwell, A., Wonacott, A.J., Wigley, D.B. The nature of inhibition of DNA gyrase by the coumarins and the cyclothialidines revealed by x-ray crystallography. *EMBO J.* 15:1412-1420, 1996.
10. Wigley, D.B., Davies, G.J., Dodson, E.J., Maxwell, A., Dodson, G. Crystal structure of an N-terminal fragment of the DNA gyrase B protein. *Nature* 351:624-629, 1991.
11. Otwinowski, Z. Oscillation data reduction program. In "Data Collection and Processing," DL/SCI/R34, compiled by L. Sawyer, N. Isaacs, and S. Bailey. SERC Daresbury Laboratory, United Kingdom. 1993:56-62.
12. Collaborative Computational Project, Number 4. The CCP4 suite: Programs for protein crystallography. *Acta Crystallogr.* D50:760-763, 1994.
13. Brünger, A.T. Free R value: A novel statistical quantity for assessing the accuracy of crystal structures. *Nature* 355:472-475, 1992.
14. Brünger, A.T., Kuriyan, J., Karplus, M. Crystallographic R factor refinement by molecular dynamics. *Science* 235:458-460, 1987.
15. Hendrickson, W.A. Stereochemically restraint refinement of macromolecular structures. *Methods Enzymol.* 115B:252-270, 1985.
16. Roussel, A., Cambillau, C. TURBO-FRODO. In "Silicon Graphics Geometry Partner Directory." Mountain View, CA: Silicon Graphics, 1989:77-78.
17. Navaza, J. AMoRe: An automated package for molecular replacement. *Acta Crystallogr.* A50:157-163, 1994.
18. Jones, T.A. A graphics model building and refinement system for macro-molecules. *J. Appl. Crystallogr.* 11:268-272, 1978.
19. Tronrud, D.E., Teneyck, L.F., Matthews, B.W. An efficient general-purpose least-squares refinement program for macromolecular structures. *Acta Crystallogr. A* 43:489-501, 1987.
20. Breeze, A.L., Kara, B.V., Barratt, D.G., Anderson, M., Smith, J.C., Luke, R.W., Best, J.R., Cartledge, S.A. Structure of a specific peptide complex of the carboxy-terminal SH2 domain from the p85 $\alpha$  subunit of phosphatidylinositol-3-kinase. *EMBO J.* 15:3579-3589, 1996.
21. Ladbury, J.E. Counting the calories to stay in the groove. *Structure* 3:635-639, 1995.
22. Wiseman, T., Williston, S., Brandts, J.F., Lin, L.-N. Rapid measurement of binding constants and heats of binding

- using a new titration calorimeter. *Anal. Biochem.* 179:131–139, 1989.
23. Laskowski, R.A., MacArthur, M.W., Moss, D.S., Thornton, J.M. PROCHECK: A program to check the stereochemical quality of protein structures. *J. Appl. Crystallogr.* 26:283–291, 1983.
24. Contreras, A., Maxwell, A. *gyrB* mutations which confer coumarin resistance also affect DNA supercoiling and ATP hydrolysis by *Escherichia coli* DNA gyrase. *Mol. Microbiol.* 6:1617–1624, 1992.
25. del Castillo, I., Vizán, J.L., Rodríguez-Sáinz, M.C., Moreno, F. An unusual mechanism for resistance to the antibiotic coumermycin A1. *Proc. Natl. Acad. Sci. USA* 88:8860–8864, 1991.
26. Holmes, M.L., Dyll-Smith, M.L. Mutations in DNA gyrase result in novo-biocin resistance in halophilic archaeobacteria. *J. Bacteriol.* 173:642–648, 1991.
27. Gormley, N.A., Orphanides, G., Meyer, A., Cullis, P.M., Maxwell, A. The interaction of coumarin antibiotics with fragments of the DNA gyrase B protein. *Biochemistry* 35:5083–5092, 1996.
28. Sugino, A., Higgins, N.P., Brown, P.O., Peebles, C.L., Cozzarelli, N.R. Energy coupling in DNA gyrase and the mechanism of action of novobiocin. *Proc. Natl. Acad. Sci. USA* 75:4838–4842, 1978.
29. Sugino, A., Cozzarelli, N.R. The intrinsic ATPase of DNA gyrase. *J. Biol. Chem.* 255:6299–6306, 1980.
30. Godfrey, J.C., Price, K.E. Structure-activity relationships in coumermycins. In "Structure-Activity Relationships Among the Semisynthetic Antibiotics." Perlman, D. (ed.). New York: Academic Press, 1977:653–718.
31. Brand, J.G., Toribara, T.Y. Induced conformational changes in novobiocin. *Mol. Pharmacol.* 8:751–758, 1972.